

Supplementary material

Synergistic Effects of Active Sites Nature and Hydrophilicity on Oxygen Reduction Reaction Activity of Pt-Free Catalysts.

Mariangela Longhi,^{a,*} Camilla Cova,^a Eleonora Pargoletti,^a Mauro Coduri,^b Saveria Santangelo,^c Salvatore Patanè,^d Nicoletta Ditaranto,^e Nicola Cioffi,^e Anna Facibeni,^f Marco Scavini^a

^aUniversità degli Studi di Milano, Dipartimento di Chimica, Via Golgi 19, 20133 Milano (Italy)

^bESRF - The European Synchrotron, 71, Avenue des Martyrs, 38043 Grenoble (France)

^cUniversità “Mediterranea”, Dipartimento di Ingegneria Civile, dell’Energia, dell’Ambiente e dei Materiali (DICEAM), Via Graziella, Loc. Feo di Vito, 89122 Reggio Calabria (Italy)

^dUniversità di Messina, Dipartimento di Scienze Matematiche e Informatiche, Scienze Fisiche e Scienze della Terra (MIFT), Viale Stagno d’Alcontres 31, 98166 Messina (Italy)

^eUniversità degli Studi di Bari "Aldo Moro", Dipartimento di Chimica, Via Orabona 4, 70125 Bari (Italy)

^fPolitecnico di Milano, Dipartimento di Energia and NEMAS - Centre for NanoEngineered MAterials and Surfaces, Via Ponzio 34/3, 20133, Milano (Italy)

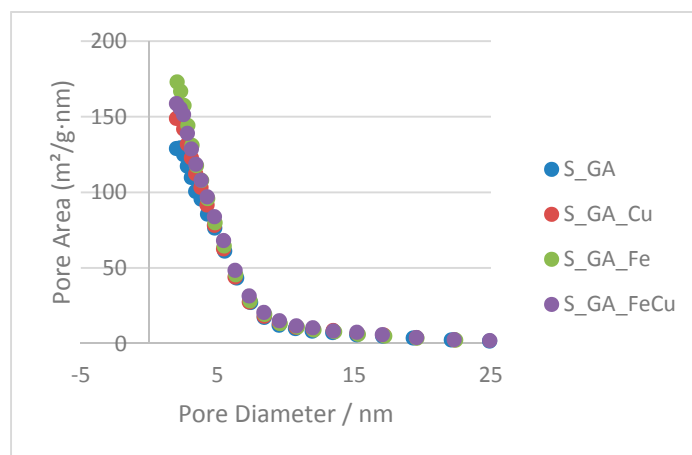


Figure S1. Porosity Distribution

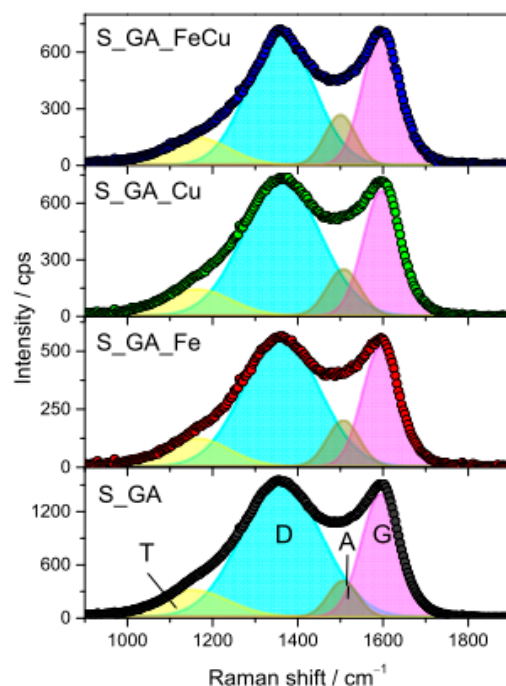


Figure S2. Results of Raman spectra decomposition. The low-frequency region of the spectra ($< 2000 \text{ cm}^{-1}$) is fitted to four bands [S1], namely the T-band ($\sim 1160 \text{ cm}^{-1}$), due to trans-poly-acetylene-like chains formed at the zigzag edges of the defective graphitic layers, the D-band ($\sim 1360 \text{ cm}^{-1}$), generated by finite size effects and by lattice defects breaking the translational symmetry of graphitic layers, the A-band ($\sim 1500 \text{ cm}^{-1}$), associated to amorphous phases connected to the ordered graphene planes through Csp^3 bonds, and the G-band ($\sim 1590 \text{ cm}^{-1}$), originating from the stretching of C=C pairs.

Table S1: Parameters inferred from Raman spectra fitting. (a) Center frequency positions (ω) and widths (γ , namely FWHM) of the main bands. (b) Relative to G-band intensity of the X-band (I_X/I_G), calculated as integrated intensity ratio. The graphitization index [S2], I_G/I_D , and the average size of the graphitic crystallites, estimated from I_G/I_D as $L_C = 560 \cdot (I_G/I_D) \cdot E_L^{-4}$ (with $E_L = 2.33 \text{ eV}$ denoting the excitation laser energy) [S3], are also reported.

(a)

| Sample | $\omega_T / \text{cm}^{-1}$ | $\gamma_T / \text{cm}^{-1}$ | $\omega_D / \text{cm}^{-1}$ | $\gamma_D / \text{cm}^{-1}$ | $\omega_A / \text{cm}^{-1}$ | $\gamma_A / \text{cm}^{-1}$ | $\omega_G / \text{cm}^{-1}$ | $\gamma_G / \text{cm}^{-1}$ |
|-----------|-----------------------------|-----------------------------|-----------------------------|-----------------------------|-----------------------------|-----------------------------|-----------------------------|-----------------------------|
| S_GA | 1151 | 203 | 1363 | 224 | 1508 | 83 | 1597 | 109 |
| S_GA_Cu | 1165 | 187 | 1364 | 215 | 1510 | 92 | 1599 | 103 |
| S_GA_Fe | 1164 | 180 | 1363 | 211 | 1509 | 90 | 1597 | 102 |
| S_GA_FeCu | 1163 | 181 | 1362 | 183 | 1502 | 86 | 1596 | 101 |

(b)

| Sample | I_T/I_G | A_D/A_G | I_A/I_G | I_G/I_D | L_C / nm |
|-----------|-----------|-----------|-----------|-----------|-------------------|
| S_GA | 0.41 | 2.27 | 0.22 | 0.44 | 8.4 |
| S_GA_Cu | 0.38 | 2.26 | 0.34 | 0.44 | 8.4 |
| S_GA_Fe | 0.42 | 2.25 | 0.34 | 0.44 | 8.4 |
| S_GA_FeCu | 0.38 | 1.82 | 0.33 | 0.55 | 10.5 |

Table S2. Lattice parameters, weight fraction (WF), average displacement parameters (U_{mean}) and fit residuals for the refinements performed on crystalline phases.

| | Sample | ZGAG_Cu | ZGAG_CuFe |
|----|------------------------------|------------|------------|
| Cu | Space group | Fm-3m | Fm-3m |
| | a/Å | 3.61711(1) | 3.61774(1) |
| | WF/% | 2.7(1) | 1.6(1) |
| C | Space group | P63mc | P63mc |
| | a/Å | 2.481(2) | 2.476(2) |
| | c/Å | 6.928(5) | 6.934(5) |
| | WF | 97.3(1) | 98.4(1) |
| | $U_{\text{mean}}/\text{Å}^2$ | 0.0064(2) | 0.0056(3) |
| | R(F2) | 0.0368 | 0.0414 |
| | RP | 0.0270 | 0.0270 |

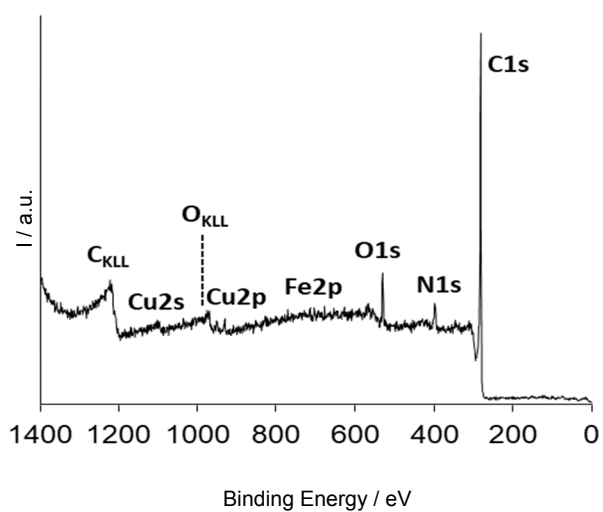


Figure S3. XPS survey of S_GA_FeCu.

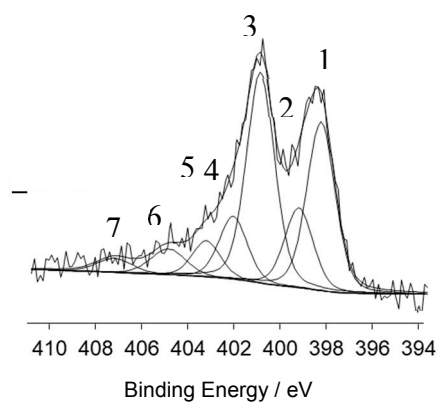


Figure S4. XPS N1s region of S_GA_FeCu. 1) Pyridinic N; 2) N_x-Me or Amine N; 3) Pyrrolic N; 4) Quaternary N; 5) Graphitic N; 6) Shake up π - π^* ; 7) Shake up π - π^*

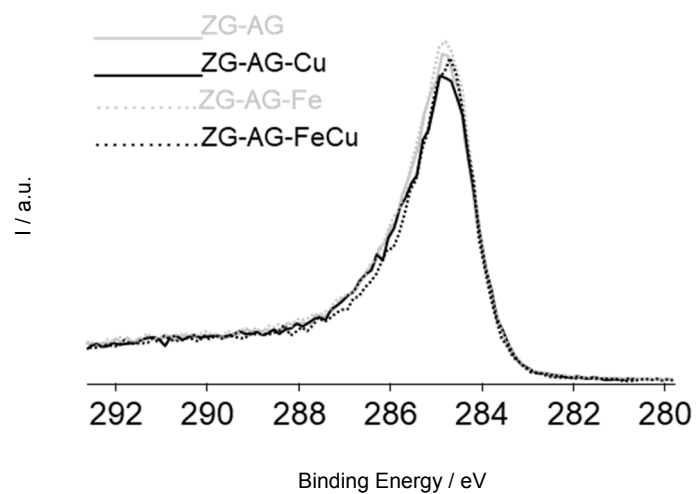


Figure S5. Superimposition of XPS C1s spectra

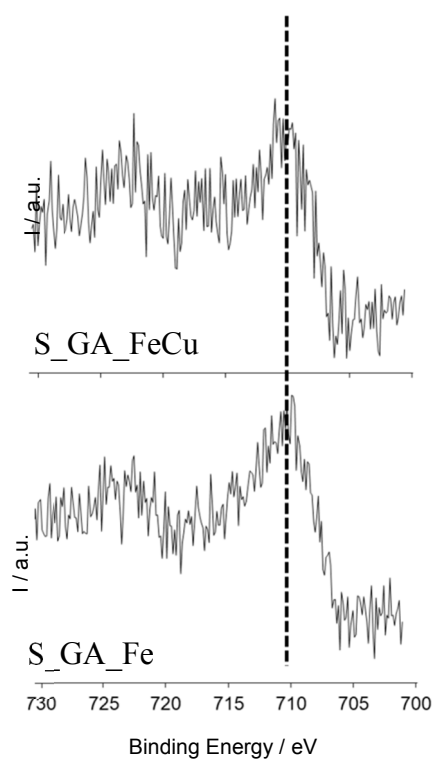


Figure S6. XPS Fe2p spectra of S_GA_FeCu and S_GA_Fe

References

- [S1] K. Bogdanov, A. Fedorov, V. Osipov, T. Enoki, K. Takai, T. Hayashi, V. Ermakov, S. Moshkalev, A. Baranov, Annealing-Induced Structural Changes of Carbon Onions: High-Resolution Transmission Electron, Microscopy and Raman Studies, *Carbon* 73 (2014) 78–86. DOI: 10.1016/j.carbon.2014.02.041.
- [S2] S. Santangelo, Functionalisation of Carbon Nanotubes by Nitric Acid Vapors Generated from Sub-Azeotropic Solution, *Surf. Interf. Analysis* 48 (2016) 17–25. DOI: DOI:10.1002/sia.5875.
- [S3] L.G. Cançado, K. Takai, T. Enoki, M. Endo, Y.A. Kim, H. Mizusaki, A. Jorio, L.N. Coelho, R. Magalhães-Paniago, M.A. Pimenta, General Equation for the Determination of the Crystallite Size L_a of Nanographite by Raman Spectroscopy, *Appl. Phys. Lett.* 88 (2006) 163106–163108. DOI: 10.1063/1.2196057.